



Contents lists available at SciVerse ScienceDirect

Spectrochimica Acta Part A: Molecular and Biomolecular Spectroscopy

journal homepage: www.elsevier.com/locate/saa

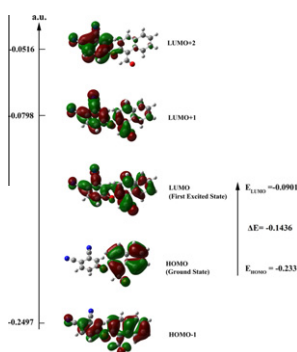
Combined experimental and theoretical approaches to the molecular structure of 4-(1-formylnaphthalen-2-yloxy)phthalonitrile

Hidayet Tereci^a, İskender Askeroğlu^a, Nesuhi Akdemir^b, İbrahim Uçar^{c,*}, Orhan Büyükgüngör^c^a Department of Physics, Faculty of Arts and Sciences, Gaziosmanpaşa University, Gaziosmanpaşa Üniversitesi, Taşlıçiftlik Yerleşkesi, 60250 Tokat, Turkey^b Department of Chemistry, Faculty of Arts and Sciences, Amasya University, 05100 Amasya, Turkey^c Department of Physics, Faculty of Arts and Sciences, Ondokuz Mayıs University, Kurupelit, TR-55139 Samsun, Turkey

HIGHLIGHTS

- ▶ The crystal structure is stabilized by weak C–H···O hydrogen-bond and π – π interactions.
- ▶ The structural and spectroscopic data of the compound was calculated using DFT and HF methods.
- ▶ Electronic absorption spectra of the title compound were predicted and good agreement with the TD-DFT method.
- ▶ Isotropic chemical shifts (¹³C and ¹H NMR) were calculated using the GIAO method.

GRAPHICAL ABSTRACT



ARTICLE INFO

Article history:

Available online 16 July 2012

Keywords:

Phthalonitrile
X-ray diffraction
FT-IR
¹³C and ¹H NMR
UV–Vis
DFT

ABSTRACT

The novel compound 4-(1-formylnaphthalen-2-yloxy)phthalonitrile, C₁₉H₁₀N₂O₂, has been synthesized and characterized by IR, UV–vis, NMR and X-ray single-crystal determination. The title compound, is built up from two planar groups (naphthalen and phthalonitrile), with a dihedral angle of 64.10(4)° between them. The crystal structure is stabilized by weak C–H···O hydrogen-bond and π – π interactions. The structural and spectroscopic data of the compound in the ground state have been calculated using density functional theory (DFT) and Hartree–Fock (HF) with the 6-31G(d,p) basis set. The vibrational study was interpreted in terms of potential energy distribution (PED). The observed wave number in FT-IR spectra was analyzed and assigned to different normal modes of the molecule. Using the TD-DFT and TD-HF methods, electronic absorption spectra of the title compound were predicted and good agreement with the TD-DFT method and the experimental determination was found. Isotropic chemical shifts (¹³C and ¹H NMR) were calculated using the gauge-invariant atomic orbital (GIAO) method. The HOMO and LUMO analyses were used to elucidate information regarding charge transfer within the molecule.

© 2012 Elsevier B.V. All rights reserved.

Introduction

Phthalonitriles have been used as starting materials for phthalocyanines [1], which are important components for dyes, pigments, gas sensors, optical limiters and liquid crystals, and which

are also used in medicine, as singlet oxygen photosensitisers for photodynamic therapy (PDT) [2]. Some phthalocyanines have been used by the petroleum industry as catalysts for the oxidation of sulfur compounds in the gasoline fraction. Applications as photoconductors in the xerographic double layers of laser printers and copy machines, and as active materials in writable disks, are also known [3]. Vibrational studies of phthalonitriles are of interest in their own right and they are extremely valuable when performing vibrational studies of larger composite molecular systems [4].

* Corresponding author. Tel.: +90 3623121919; fax: +90 3624576081.

E-mail address: iucar@omu.edu.tr (I. Uçar).

Computational Chemistry, which is also called Molecular Modeling, is based on a set of techniques for investigating chemical problems on a computer. Some of the subjects that are commonly investigated computationally are the molecular optimization, the IR, UV and NMR spectra, the EPR parameters, the energies of molecules and transitions states, chemical reactivity and the physical properties of substances [5–8]. Density functional theory (DFT) is a quantum mechanical theory used in physics and chemistry to investigate the electronic structure of many-body systems, in particular atoms, molecules, and the condensed phases [9,10]. By means of DFT, the properties of a many-electron system can be determined by using functionals, i.e. functions of another function, which in this case is the spatially dependent electron density. The development of better exchange–correlation functionals made it possible to calculate many molecular properties with comparable accuracies to traditional correlated *ab initio* methods, with more favorable computational costs [11].

In our ongoing research, we have recently synthesized some phthalonitriles derivatives and their structures have been reported [12]. In this article, we present the synthesis, crystal, molecular, electronic structures, and spectroscopic characterization of 4-(1-formylnaphthalen-2-yloxy)phthalonitrile. In order to help to make further investigate on the properties of the synthesized compounds density functional theory (DFT) and HF calculations were carried out.

Experimental and theoretical methods

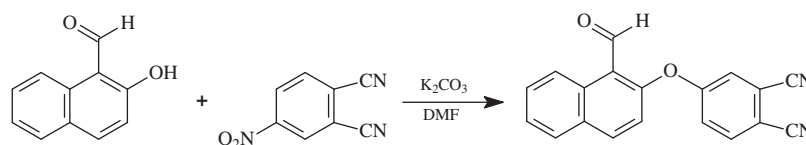
General method

2-Hydroxy-1-naphthaldehyde was purchased from the Fluka. 4-Nitrophthalonitrile was synthesized according to the reported procedure [13]. All other reagents and solvents were of reagent-grade quality and were obtained from commercial suppliers. All solvents were dried and purified as described by Perin and Armarego [14]. The solvents were stored over molecular sieves (4 Å). The homogeneity of the products was tested by TLC (SiO₂ or Al₂O₃). The IR spectra were recorded in the 4000–400 cm⁻¹ region using KBr pellets on a Vertex 80 V Bruker FT-IR spectrophotometer. Electronic absorption spectra were measured on a Unicam UV–VIS spectrometer in the range 900–200 nm. ¹H NMR and ¹³C NMR studies were made on a Bruker AC-200 FT-NMR spectrometer.

Synthesis

Synthesis of 4-(1-formylnaphthalen-2-yloxy)phthalonitrile

2-Hydroxy-1-naphthaldehyde (0.90 g, 5.23 mmol) and 4-nitrophthalonitrile (0.82 g, 4.74 mmol) were dissolved in dry dimethylformamide (60 ml) with stirring under N₂. Dry fine-powdered potassium carbonate (2.00 g, 14.49 mmol) was added in portions (10 × 1.5 mmol) every 10 min. The reaction mixture was stirred for 48 h at room temperature and poured into ice-water (150 g). The product was filtered off and washed with water until the filtrate was neutral. Recrystallization from ethanol solution gave a brown product (yield 0.28 g, 19.86%). Single crystals (Scheme 1) were obtained from DMF solution of the compound via slow evaporation at room temperature (m.p. 451–454 K).



Scheme 1.

¹H NMR (CDCl₃): δ: ppm: 7.16 (d), 7.26–7.95 (m), 8.20 (d), 9.24 (d), 10.73 (s); ¹³C-NMR (CDCl₃): δ: ppm: 110.37, 114.63, 115.00, 118.20, 119.20, 121.63, 121.70, 122.04, 125.52, 127.25, 128.66, 130.53, 130.13, 131.72, 135.76, 138.09, 157.23, 161.09, 189.88.

Crystal structure determination and refinement

The diffraction data were collected on a STOE IPDSII image plate detector using Mo K α radiation ($\lambda = 0.71073$ Å, $T = 297$ K). The technique used was $w-2\theta$ scan mode with limits 2.7–27.5°. A summary of the key crystallographic information is given in Table 1. Data collection: Stoe X-AREA [15]. Cell refinement: Stoe X-AREA [15]. Data reduction: Stoe X-RED [15]. The structure was solved by direct-methods using SHELXS-97 [16] and anisotropic displacement parameters were applied to non-hydrogen atoms in a full-matrix least-squares refinement based on F² using SHELXL-97 [16]. All H atoms attached to carbon atoms were positioned geometrically and refined by a riding model with U_{iso} 1.2 times that of attached atoms. Molecular drawings were obtained using DIAMOND 3.0 (demonstrated version) [17].

Computational methods

The crystal structure was used as an initial molecular geometry. Quantum chemical calculations are performed with GAUSSIAN 03 program packages [18]. The output files are visualized by means of GAUSSIAN VIEW 03 software [19]. The geometry of neutral form of title compound was optimized at two levels of theory: density functional theory (DFT) and Hartree–Fock Theory using the 6-31G(d,p) [20,21] basis set, respectively. The DFT method employed is B3LYP, which combines Becke's three-parameter non-local exchange function with the correlation function of Lee et al. [22,23]. Molecular geometry of the studied structure was fully optimized by the force gradient method using Berny's algorithm.

The electronic spectrum of title complex was calculated with the TDDFT and TDHF method starting from the ground-state geometry optimized in the gas phase. The solvent (ethanol) effect was stimulated using the polarizable continuum model (PCM). The calculated vibrational frequencies were carried out using the DFT/B3LYP and HF level of theories. For the structures, the stationary points found on the molecule potential energy hypersurfaces were characterized using standard analytical harmonic vibrational analysis. The absence of the imaginary frequencies, as well as of negative eigenvalues of the second derivative matrix, confirmed that the stationary points correspond to minima of the potential energy hypersurfaces. A detailed interpretation of the vibration spectra of this compound has been made on the basis of the calculated potential energy distribution (PED) using the VEDA 4 program.

Results and discussion

Molecular structure of 4-(1-formylnaphthalen-2-yloxy)phthalonitrile

The crystal structure of (1) is shown in Fig. 1 and selected bond distances and angles are summarized in Table 2. The compound (1), crystallizes in the monoclinic space group C2/c with eight molecules in the unit cell. It contains two ring systems, naphthalen and

Table 1
Crystal data and structure refinement for 4-(1-formylnaphthalen-2-yloxy)phthalonitrile.

Formula	C ₁₉ H ₁₀ N ₂ O ₂
Formula weight (g)	298.29
Temperature (K)	297 K
Wavelength (Mo Å)	0.71073
Crystal system	Monoclinic
Space group	C2/c
Unit cell dimensions	
<i>a</i> , <i>b</i> , <i>c</i> (Å)	27.976(5), 8.350(5), 14.418(5)
β (°)	117.891(5)
Volume (Å ³)	2977(2)
<i>Z</i>	8
Calculated density (g cm ⁻³)	1.331
μ (mm ⁻¹)	0.088
<i>F</i> (0,0,0)	1232.0
Crystal size (mm)	0.4 × 0.3 × 0.1
θ Ranges (°)	2.7–27.5
Index ranges	–33 ≤ <i>h</i> ≤ 36 –9 ≤ <i>k</i> ≤ 10 –18 ≤ <i>l</i> ≤ 18
Reflections collected	25745
Independent reflections	3404 [<i>R</i> _(int) = 0.023]
Reflection observed (<i>I</i> > 2 σ)	2355
Absorption correction	Integration
Refinement method	Full-matrix least-squares on <i>F</i> ²
Data/restraints/parameters	3404/0/209
Goodness-of-fit on <i>F</i> ²	0.973
Final <i>R</i> indices [<i>I</i> > 2 σ (<i>I</i>)]	0.037
<i>R</i> indices (all data)	0.060
Largest diff. Peak and hole (e Å ⁻³)	0.13 and –0.13

phthalonitrile, linked by an O atom, forming non-planar molecular structure. The phthalonitrile ring exhibits normal geometry and is planar. The two cyano groups deviate from this plane by 0.009(1) and 0.008(1) Å at atoms N2 and N1, respectively. The naphthalen system is also planar, with a maximum deviation of 0.033(3) Å for atom C17. The phthalonitrile and naphthalen groups make a dihedral angle of 64.10(4)°. The C≡N bond lengths [N1≡C1 = 1.139(2) Å and N2≡C2 = 1.137(2) Å] compare well with values reported in the literature [24,25]. As expected, the N≡C–C angles [N1≡C1–C4 = 179.2(2)° and N2≡C2–C3 = 178.9(2)°] are linear.

The crystal packing is formed by weak intra and intermolecular hydrogen bonding (C–H...O) interactions (Fig. 2, Table 3). Apart from these, there is also symmetry-related weak slipping face to face π – π stacking interaction between the two phenyl rings of

Table 2
Selected structural parameters by X-ray and theoretical calculations for compound (1).

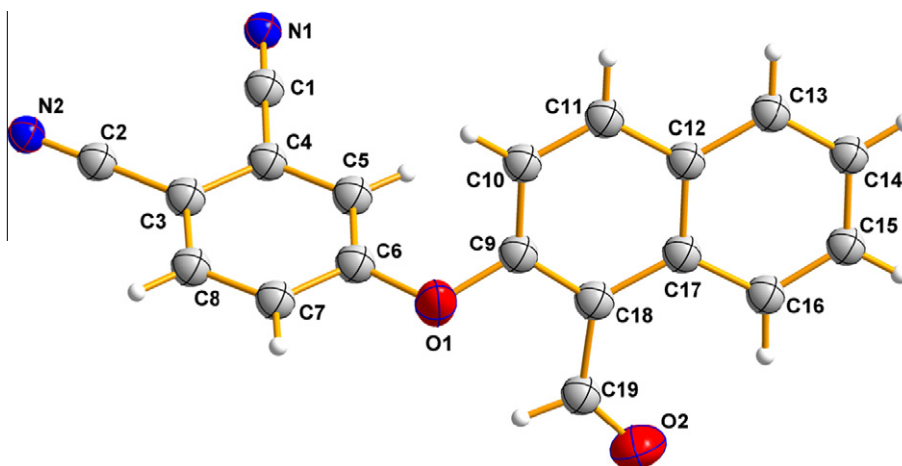
	Experimental	Calcd.	
		HF	DFT/B3LYP
<i>Bond lengths</i> (Å)			
N1–C1	1.13891(2)	1.13931	1.14621
N2–C2	1.13684(3)	1.13975	1.14699
C6–C7	1.37882(3)	1.38257	1.38593
O1–C6	1.36783(2)	1.38018	1.37744
C16–C17	1.41543(3)	1.42022	1.42201
O2–C19	1.19665(3)	1.21407	1.21911
C12–C17	1.41814(2)	1.41137	1.41679
<i>Bond angles</i> (°)			
C2–C3–C4	120.819(15)	120.978	121.268
N1–C1–C4	179.217(19)	179.374	179.121
O1–C6–C5	123.081(15)	122.853	122.866
O1–C9–C18	117.495(13)	118.843	118.765
C12–C17–C18	118.638(16)	118.849	118.756
N2–C2–C3	178.960(19)	179.214	179.024
O1–C6–C7	115.543(14)	116.446	116.101
C16–C17–C18	123.899(14)	122.956	123.368

naphthalen group (C9–C10–C11–C12/C17–C18; Slippage distance between the two phenyl rings is 1.129 Å). The centroid to-centroid and centroid-to-plane distances between the phenyl rings are 3.791(2) and 3.412(5) Å, respectively. The closest interatomic distance between these ring planes is [C9...C10(1/2 – *x*, 1/2 – *y*, –*z*)] 3.488(3) Å.

Optimized structure

Ab initio calculations were performed on compound (1) at DFT/B3LYP/6-31G(d,p) and HF/6-31G(d,p) level of theory. Some optimized geometric parameters of (1) are listed in Table 2. A superposition of the molecular structure of compounds as established by quantum mechanical calculations and X-ray study shows an excellent agreement (Fig. 3). Comparing the theoretical data with the experimental ones indicates that optimized bond lengths and angle values are slightly different with the experimental results. It should be noted that the geometry of the solid state structure is subject to intra and intermolecular interactions, such as hydrogen bonding and van der Waals interactions.

As seen in Table 2, the largest discrepancies between the calculated and experimental geometrical parameters are observed for C–H. Large deviation from experimental C–H bond distances may

**Fig. 1.** The molecular structure of 4-(1-formylnaphthalen-2-yloxy)phthalonitrile, showing the atom-numbering scheme. Displacement ellipsoids are drawn at the 40% probability level and H atoms are shown as small spheres of arbitrary radii.

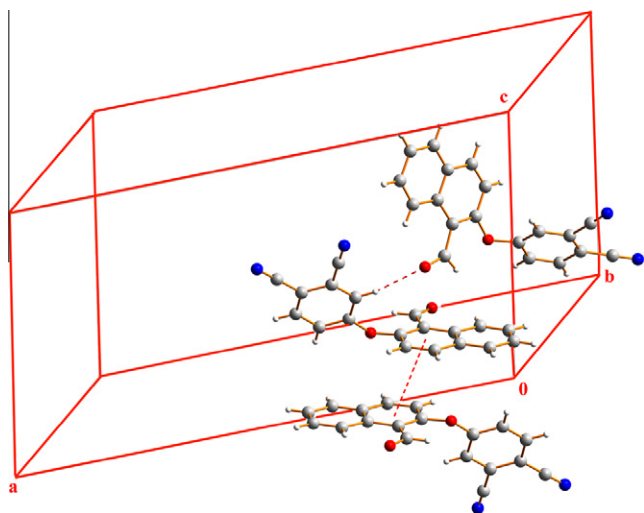


Fig. 2. A view of the packing of 4-(1-formylnaphthalen-2-yloxy)phthalonitrile, showing hydrogen bonding and π - π interactions as dashed lines.

Table 3
Hydrogen bonding interactions for 4-(1-formylnaphthalen-2-yloxy)phthalonitrile.

D-H...A	D-H	H...A	D...A	D-H...A
C5-H3...O2 ⁱ	0.93	2.45	3.359(3)	167
C16-H9...O2	0.93	2.27	2.906(3)	125
C19-H10...O1	0.93	2.31	2.708(3)	105

Symmetry code: (i) = 1/2 - x, 1/2 + y, 1/2 - z.

arises from the low scattering factors of hydrogen atoms in the X-ray diffraction. Several authors have been reported that the HF methods under estimate some bond length and DFT/B3LYP methods predicts bond lengths which are systematically too long, especially C-H bond lengths [26–29].

The largest difference between experimental and calculated DFT bond length is 0.022 Å (C2–C3) for, whereas this difference for HF method is 0.017 Å (C2–C3), which suggest that the calculational precision is satisfactory [30]. These theoretical results indicate that the HF method gives geometric parameters, which are much closer to experimental ones. Similar situation is also observed for calculated bond angles with HF and DFT method.

Vibrational assignments

Some primary calculated harmonic frequencies are listed in Table 4, together with experimentally determined frequencies (Fig. 4). Calculated vibrational frequencies of (1) at DFT/B3LYP and HF levels were scaled by 0.96 and 0.89, respectively [31]. According to the theoretical calculations, both the optimized molecular structures belong to the C1 point group as it does not display any special symmetry. As a result of this all the normal modes of both compounds are infrared active. The vibrational assignments have been done on the basis of relative intensities,

line shape, the VEDA 4 program and the animation option of GAUSS VIEW 3.0. The potential energy distribution is also supporting the present study. The computed intensities show marked deviations from the observed values, since computed wavenumbers correspond to the isolated molecular state, whereas the observed wavenumbers correspond to the solid state spectra.

The heterocyclic aromatic compounds and its derivatives are structurally very close to benzene. These compounds shows the presence of C–H stretching vibration in the region 3100–3000 cm^{-1} , which is the characteristic region for the ready identification of C–H stretching vibrations [32]. In this region, the nature of the substituents does not make any appreciable change [33]. In this study, first ten vibrations are assigned to C–H stretching, which correspond to stretching modes of the C–H of ring and aldehyde units. All modes are almost pure stretching vibrations 100% PED terms. The C–H in-plane bending wavenumbers appear in the range of 1000–1500 cm^{-1} and C–H out-of-plane bending vibration in the range of 700–1000 cm^{-1} . The in-plane C–H bending vibrations were assigned in the range that mentioned above and according to their PED; they are described as mixed modes, generally with C–C vibrations. The C–C stretching vibrations show absorption in the region 1300–700 cm^{-1} [34]. Accordingly, the bands observed at 1279 and 1066 and 709 cm^{-1} in FT-IR spectra have been assigned to CC stretching vibrations which are well comparable with the computed values. The theoretically calculated CCC bending vibration has been found to be consistent with the recorded spectral values and is listed in Table 4 with the contribution of 30–23% PED.

The sharp band in the region of 2210–2270 cm^{-1} is easily assigned to the characteristic $\text{C}\equiv\text{N}$ stretching mode [35]. In previously reported similar studies were assigned the cyano stretching vibration in the range of 2229–2249 cm^{-1} for hydroxy-containing phthalonitrile model compounds [4,36–38]. In this study, the strong band at 2230 cm^{-1} in FT-IR spectrum and calculated band at 2212–2216 cm^{-1} (DFT), 2276–2281 cm^{-1} (HF) are assigned to $\text{C}\equiv\text{N}$ stretching vibrations which have good correlation with literature.

The C=O/C–O band is reasonably easy to be recognized due to its high intensity [39]. In this study, the band observed at 1674 cm^{-1} in FT-IR spectra (mode No.13) has been assigned to C=O stretching vibration, with the contribution of 45% PED. The band observed at 990 cm^{-1} in FT-IR spectrum is assigned to C–O stretching vibration (mode No. 45), which is in good agreement with the theoretically calculated values.

UV-vis spectrum and electronic properties

The UV-vis electronic spectra of compound (1) in ethanol solution were recorded within 200–800 nm range. The theoretical electronic excitation energies, oscillator strengths and nature of the first 20 spin-allowed singlet-singlet electronic transitions were calculated by the TD-DFT/PCM method for the above solvents. The major contributions of the transitions were designated with the aid of SWizard program [40]. The experimental and calculated results of UV-vis spectral data were compared in Table 5. Each

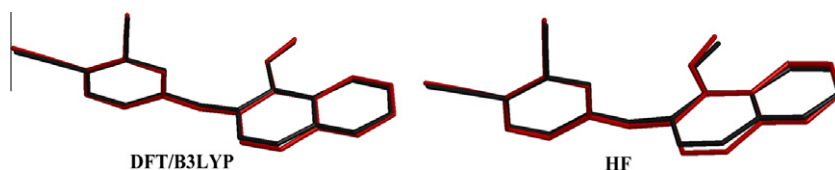
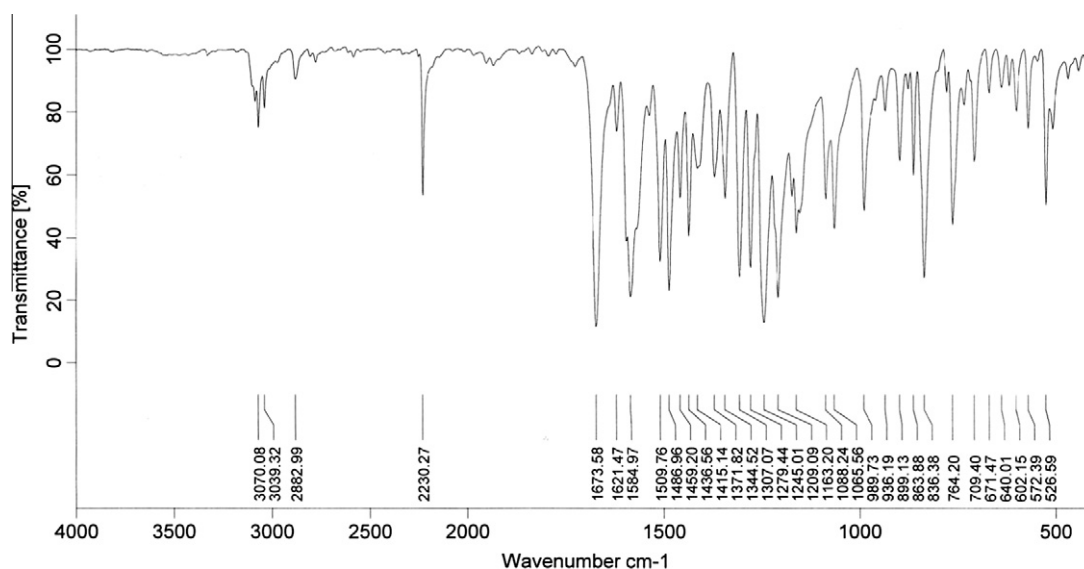


Fig. 3. Atom-by-atom superimposition of the 4-(1-formylnaphthalen-2-yloxy)phthalonitrile calculated (red) over the X-ray structure (black) (for interpretation of the references to color in this figure legend, the reader is referred to web version of this article).

Table 4

Comparison of the observed and calculated vibrational spectra of compound (1).

Experimental FT-IR (cm ⁻¹)	DFT/B3LYP Scaled (cm ⁻¹)	HF/6-31 G(d,p) Scaled (cm ⁻¹)	PED (≥10%) Assignments
3070	3141	3078	ν CH _{R3} (98)
3040	3120	3037	ν CH _{R1} (99)
2882	2937	2942	ν CH _{Aldehit} (100)
2230	2216	2281	ν C≡N (85) + ν CC (12)
1674	1621	1674	ν CO (45)
1621	1604	1629	ν CO (23) + ν {CH _{R1} + CH _{R2} + CH _{R3} } (36)
1584	1584	1607	ν {CH _{R1} + CH _{R2} } (33)
1509	1504	1504	β (HCC _{R2}) (11) + ν {CH _{R2} + CH _{R3} } (10)
1486	1479	1495	β (HCC _{R1}) (22) + β (HCC _{R2}) (26) + β (CCC _{R1}) (10)
1459	1456	1463	β (HCC _{R3}) (19) + β (HCC _{R2}) (12) + β (HCC _{alde}) (11) + β (HCC _{R1}) (15)
1436	1431	1432	ν CC _{R3} (14) + ν CC _{R2} (14) + β (HCC _{alde}) (12)
1415	1403	1400	β (HCO) _{Ald} (66)
1371	1368	1360	ν CC _{R2} (14) + ν CC _{R3} (14) + β (HCC _{alde}) (12)
1344	1360	1341	ν CC _{R2} (14) + ν CC _{R3} (14)
1307	1305	1289	ν CC _{R1} (77)
1279	1280	1272	ν CC _{R1} (15) + β (HCC _{R1}) (27) + β (HCC _{R2}) (29)
1245	1274	1247	ν CC _{R3} (15) + β (HCC _{R3}) (27) + β (HCC _{R1}) (29)
1209	1227	1210	ν CC _{R1} (21) + ν CO (21)
1163	1166	1153	β (HCC _{R3}) (17) + β (HCC _{R2}) (11) + β (HCC _{R1}) (13)
1088	1083	1081	ν CC _{R1} (10) + β (CCC _{R1}) (10) + β (HCC _{R1}) (20)
1065	1057	1071	ν {CC _{R2} + CC _{R3} } (19) + β {(CCC _{R2}) + (CCC _{R3})} (28)
989	976	1021	γ CH _{R3} (23) + γ CH _{R2} (34)
936	916	949	ν CC _{R1} (11) + ν CC _{R2} (12) + ν CO (14)
899	896	920	γ CH _{R1} (72)
863	855	885	β (CCC _{R3}) (31) + β (CCO) (12) + β (CCC _{R2}) (14)
836	843	860	γ CH _{R1} (78)
764	759	784	γ CH _{R3} (22) + γ CH _{R2} (40)
709	720	720	ν CC _{R1} (16) + β (CCC _{R1}) (39)
671	666	672	β (OCC) (11) + γ OCCC (15)
640	633	640	β (OCC) (11)
602	618	629	γ OCCC (20) + γ CCCC _{R1} (12)
572	568	566	β (CCO) (14) + β {(CCC _{R1}) + (CCC _{R2}) + (CCC _{R3})} (14)
526	525	535	γ {(CCC _{R1} + CCC _{R2} + CCC _{R3})} (27)
509	508	513	β {(CCC _{R1} + CCC _{R2} + CCC _{R3})} (10) + β (CCC) (13)
408	410	416	γ CCCC _{R1} (13) + γ CCCC _{R2} (13) + γ CCCC _{R3} (21)

R1: phthalonitrile ring; R2 and R3: naphthalene rings; ν : stretching; β : in-plane bending; γ : out-of-plane bending.**Fig. 4.** The experimental Infrared spectra of the present 4-(1-formylnaphthalen-2-yloxy)phthalonitrile.

calculated transition is represented by a Gaussian function $y = ce^{-bx^2}$ with the height c equal to the oscillator strength and b equal to 0.04 nm^{-2} . The predicted absorption wavelengths using the HF level of theory for title compound are not corresponding

to the experimental results; therefore these results are not discussed in this part.

The analysis of the wave function indicates that the electron absorption corresponds to the transition from the ground to the

Table 5
Calculated electronic transitions for 4-(1-formylnaphthalen-2-yloxy)phthalonitrile with TD-DFT and TD-HF methods.

Exper. λ (nm)	DFT/B3LYP				HF/6 31G(d,p)			
	λ (nm)	Osc. strength	E (eV)	Major contributions	λ (nm)	Osc. strength	E (eV)	Major contributions
386	379	0.0092	3.27	H-2 \rightarrow L (44%) H-1 \rightarrow L (22%)	-	-	-	-
	355	0.0786	3.49	H \rightarrow L (88%)	-	-	-	-
329	331	0.0653	3.74	H \rightarrow L+1 (92%)	-	-	-	-
	326	0.2830	3.80	H-1 \rightarrow L (62%) H-2 \rightarrow L (22%)	-	-	-	-
260	276	0.0564	4.48	H \rightarrow L+2 (78%) H-3 \rightarrow L (11%)	246	0.2921	5.03	H \rightarrow L (50%) H \rightarrow L+1 (33%)
	253	0.2521	4.88	H-3 \rightarrow L+1 (43%) H-1 \rightarrow L+2 (39%)	232	0.2223	5.34	H-1 \rightarrow L (44%) H-1 \rightarrow L+1 (21%)
	242	0.1044	5.11	H-2 \rightarrow L+2 (48%) H-5 \rightarrow L (25%)	-	-	-	-
215	238	0.1368	5.21	H-5 \rightarrow L (41%) H \rightarrow L+3 (16%)	214	0.4337	5.77	H-2 \rightarrow L (36%) H-2 \rightarrow L+1 (24%)

H: HOMO.

L: LUMO.

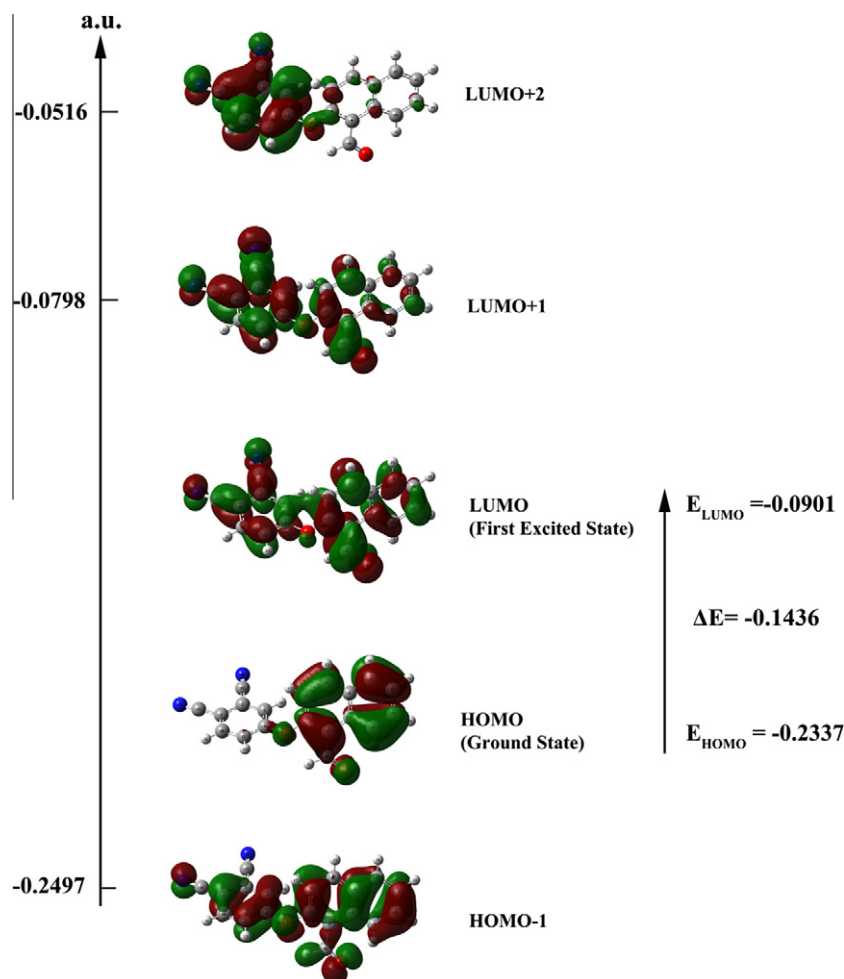


Fig. 5. Molecular orbital surfaces and energy levels using the DFT/B3LYP method for the, HOMO, HOMO–1, LUMO and LUMO + 1/2 of 4-(1-formylnaphthalen-2-yloxy)phthalonitrile.

first excited state. It is mainly described by one-electron excitation from the highest occupied molecular orbital (HOMO) to the lowest unoccupied molecular orbital (LUMO). The HOMO energy characterizes the ability of electron giving, LUMO characterizes the ability of electron accepting, and the gap between HOMO and LUMO characterizes the molecular chemical stability [41]. The several contours of occupied and unoccupied MOs (active in the electronic states) are presented in Fig. 5.

According to the TD-DFT, the predicted electronic spectrum at bands between the 200–400 nm is assigned to the electronic

transitions from the HOMO and lower occupied MOs to LUMO and higher unoccupied MOs. Molecular orbital coefficients analyses based on DFT/B3LYP optimized structure indicate that frontier molecular orbitals are mainly composed of p atomic orbitals, so electronic transitions are mainly derived from the $n \rightarrow \pi^*$ and $\pi \rightarrow \pi^*$ transitions. It is clear from Fig. 5 that while the HOMO and HOMO–2 orbitals are delocalized on the naphthalene and aldehyde group, in LUMO and LUMO+1 electron cloud is completely delocalized on whole compound. The HOMO could be characterized as a π -bonding (between a pair of naphthalene ring atoms)

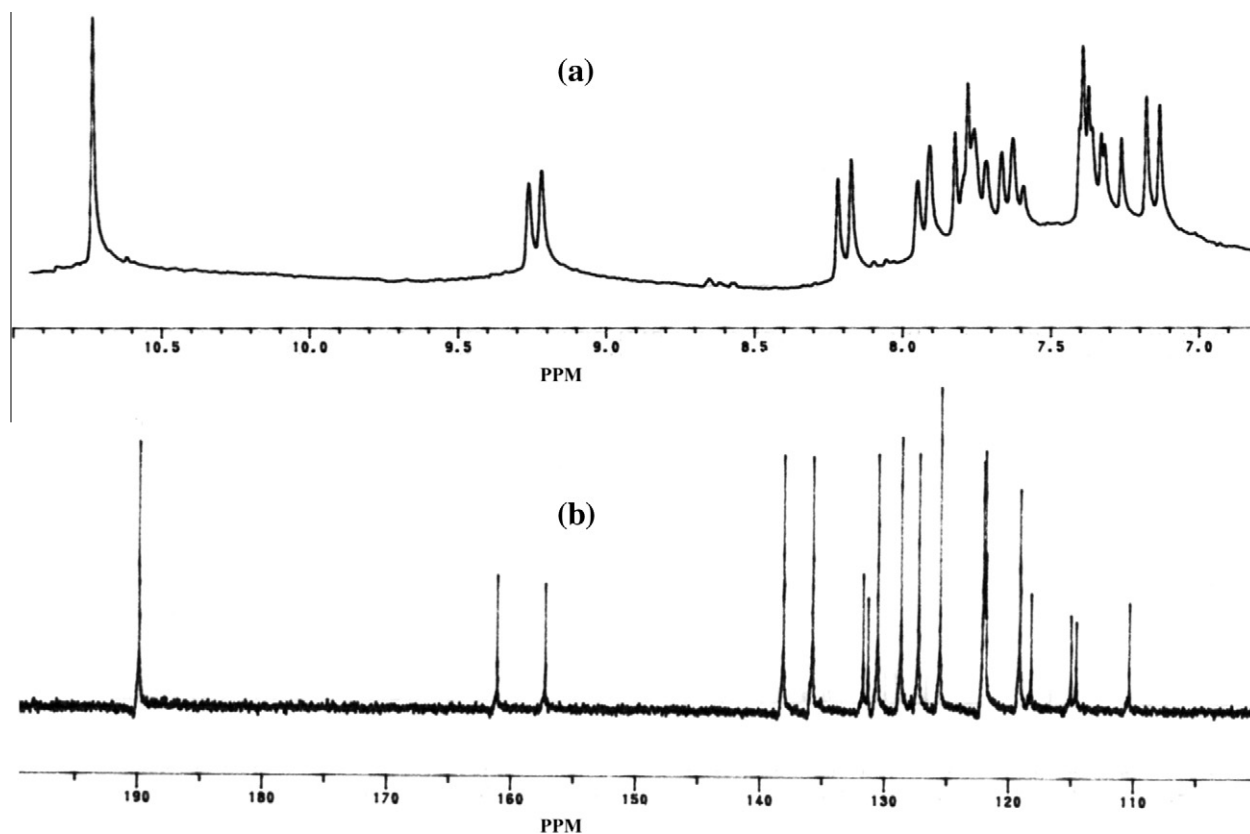


Fig. 6. The experimental ^1H (a) and ^{13}C (b) NMR spectra of 4-(1-formylnaphthalen-2-yloxy)phthalonitrile in CDCl_3 solution.

Table 6

Experimental and theoretical, ^1H and ^{13}C isotropic chemical shifts (δ) and magnetic isotropic shielding constants (σ) (with respect to TMS) of compound (1) by DFT/B3LYP method.

Atom	Gaseous		DMSO		Water		CDCl_3		δ Exp. (CDCl_3)
	δ Calcd.	σ Calcd.	δ Calcd.	σ Calcd.	δ Calcd.	σ Calcd.	δ Calcd.	σ Calcd.	
H3	6.07	25.81	6.48	25.40	6.55	25.32	6.34	25.53	7.13
H14	6.07	25.79	6.60	25.27	6.61	25.26	6.42	25.45	7.17
H7	6.69	25.20	7.05	24.83	7.05	24.83	6.95	24.92	7.26
H1	6.69	25.16	7.25	24.64	7.24	24.65	7.09	24.79	7.31
H6	6.78	25.10	7.25	24.63	7.24	24.63	7.09	24.78	7.32
H8	6.97	24.95	7.25	24.62	7.24	24.62	7.18	24.69	7.33
H2	6.97	24.90	7.50	24.38	7.49	24.38	7.34	24.53	7.36
H5	6.97	24.87	7.59	24.28	7.60	24.27	7.42	24.46	7.41
H9	9.33	22.55	9.10	22.78	9.09	22.78	9.18	22.70	9.24
H10	11.08	20.79	11.00	20.88	11.00	20.88	11.01	20.86	10.73
C3	99.67	82.78	97.96	84.49	97.88	84.58	98.41	84.05	110.37
C10	101.72	80.74	103.22	79.24	103.38	79.07	102.59	79.87	111.63
C1	102.51	79.95	104.50	77.96	104.51	77.95	104.37	78.09	115.00
C2	102.70	79.76	105.19	77.27	105.33	77.12	104.85	77.61	118.20
C4	105.60	76.86	105.78	76.68	105.91	76.55	104.94	77.52	119.20
C5	106.23	76.23	107.35	75.14	107.34	75.12	106.78	75.67	121.63
C18	107.32	75.14	107.35	75.09	107.65	74.81	107.37	75.09	121.70
C7	107.42	75.04	110.17	72.29	110.10	72.36	109.46	73.00	122.04
C16	111.25	71.21	110.51	71.95	110.44	72.02	111.27	71.19	125.52
C14	112.58	69.88	111.44	71.02	111.37	71.08	111.45	71.01	127.25
C13	112.79	69.67	114.11	68.34	114.13	68.33	113.60	68.86	128.66
C12	115.88	66.58	116.10	66.38	116.07	66.41	116.07	66.39	130.13
C15	115.94	66.52	116.10	66.35	116.07	66.40	116.16	66.30	130.53
C17	116.63	65.83	116.10	66.34	116.07	66.35	116.30	66.16	131.72
C8	120.35	62.11	122.60	59.87	122.50	59.96	121.99	60.47	135.76
C11	122.13	60.33	125.42	57.03	125.43	57.03	124.43	58.04	138.09
C9	144.67	37.79	146.65	35.82	146.79	35.67	145.96	36.50	157.23
C11	145.30	37.16	146.65	35.81	146.87	35.59	146.28	36.18	161.09
C19	181.18	1.27	183.88	-1.42	184.06	-1.59	183.02	-0.55	189.88

Table 7
Selected interactions between “filled” (donors) Lewis-type NBOs and “empty” (acceptor) non-Lewis NBOs.

Donor Lewis Type NBOs	Occupancy	Acceptor non Lewis NBOs	$E^{(2)}$ (kJmol ⁻¹) ^a	$E(j)-E(i)$ (kJmol ⁻¹) ^b
σ (O2–C19)	1.99	π^* (C18–C17)	26.16	971.41
π (C18–C17)	1.69	π^* (O2–C19)	89.32	708.88
π (C7–C8)	1.66	π^* (C5–C6)	93.38	708.88
π (C5–C6)	1.63	π^* (C7–C8)	71.73	761.41
Selected occupancy of NBOs and hybrids calculated for title compound				
Donor Lewis Type NBOs	Occupancy	Hybrid	AO(%) ^c	Acceptor non Lewis NBOs
σ (C18–C17)	1.97	sp ^{1.96} (C18)	s(33.81%)p(66.19%)	σ^* (C18–C17)
		sp ^{1.55} (C17)	s(39.27%)p(60.70%)	
π (C18–C17)	1.69	sp ^{1.0} (C18)	s(0.01%)p(99.99%)	π^* (C18–C17)
		sp ^{99.9} (C17)	s(0.03%)p(99.97%)	
σ (C11–C12)	1.97	sp ^{1.76} (C11)	s(36.23%)p(63.77%)	σ^* (C11–C12)
		sp ^{1.79} (C12)	s(35.78%)p(64.22%)	
σ (C7–C8)	1.97	sp ^{1.82} (C7)	s(35.49%)p(64.53%)	σ^* (C7–C8)
		sp ^{1.82} (C8)	s(35.47%)p(64.53%)	
σ (C5–C6)	1.97	sp ^{1.61} (C5)	s(38.25%)p(61.75%)	σ^* (C5–C6)
		sp ^{1.92} (C6)	s(34.28%)p(65.72%)	
π (C5–C6)	1.63	sp ^{1.0} (C5)	s(0.01%)p(99.99%)	π^* (C5–C6)
		sp ^{1.0} (C6)	s(0.01%)p(99.99%)	

^a Second order interaction energy (stabilization energy).

^b Energy difference between donor and acceptor *i* and *j* NBO orbitals.

^c Percentage contribution of atomic orbitals in NBO hybrid.

and nonbonding molecular orbital (aldehyde oxygen atom). Finally, the LUMO and LUMO 1/2 exhibit a π -antibonding character between some pair of phthalonitrile and naphthalene groups.

¹³C and ¹H NMR calculations

In order to provide an unambiguous assignment of ¹³C and ¹H NMR spectra of compound (1) (Fig. 6), we undertook a series of NMR calculations using GIAO approximation, and the results of these calculations are shown in Table 6. The default PCM model provided by GAUSSAIN03 was also tested in order to describe the influence exerted by solvent on the NMR spectra of the given compound. The isotropic shielding values were used to calculate the isotropic chemical shifts (δ) with respect to tetramethylsilane (TMS), ($\delta_{\text{iso}}^X = \sigma_{\text{iso}}^{\text{TMS}} - \sigma_{\text{iso}}^X$). Comparison between experimental and theoretical NMR chemical shifts provides practical information on the chemical structure and conformation of compounds. It is clear from Table 6 that the agreement with experimental data is good, even the trends in relative values are well reproduced. The largest differentiation for the chloroform solution in ¹³C chemical shifts is observed for C14, amounting to about 16 ppm. The differentiation found in ¹H, on the other hand, is only of a few tenths of ppm. Signals for protons were observed at 7.13–10.73 ppm. Since H atom is the smallest of all atoms and mostly localized on the periphery of molecules, their chemical shifts would be more susceptible to intermolecular interactions in the aqueous solutions as compared to that for other heavier atoms.

Natural bond orbital analysis

The natural bond orbital (NBO) calculation of compound (1) was performed using NBO 3.1 program implemented in the GAUSSIAN03 package at the DFT/B3LYP/6-31G(d,p) level. The NBO analysis can be used to investigate the charge transfer or estimate delocalization of electron density between occupied Lewis-type orbitals and formally unoccupied non-Lewis NBOs, which corresponds to a stabilizing donor–acceptor interaction [42]. According to the NBO results, the electronic configuration of N1 atom in compound is [core] 2S^{1.61}2p^{3.64}, 1.99 core electrons, 5.24 valence electrons (on 2s, 2p atomic orbitals) and 0.007 Rydberg electrons. This gives the total of 7.25, which is consistent with the calculated

natural charge [–0.25] on the N1 atom. The largest negative charges are located on the oxygen atoms O1 (–0.51 e) and O2 (–0.52 e) for title compound.

Hyperconjugation is the interaction of the electrons in a sigma bond with an adjacent empty (or partially filled) non-bonding p-orbital or antibonding π orbital or filled π orbital, to give an extended molecular orbital that increases the stability of the system when these orbitals are properly oriented. Second order perturbation theory allows making conclusions about the strength the hyperconjugative interaction energy. The larger the second order interaction energy ($E^{(2)}$) value, the more intensive is the interaction between electron donors and electron acceptors, i.e., the more donating tendency from electron donors to electron acceptors and the greater the extent of conjugation of the whole system. These interactions can be identified by finding the increase in electron density (ED) in anti-bonding orbital that weakens the respective bonds. The NBO analysis results show that the σ (O2–C19) participates as donor and the π^* (C18–C17) antibond as acceptor [σ (O2–C19) \rightarrow π^* (C18–C17)], and the charge transfer energy value is 971.4 kJ/mol. This interaction weakens the C18–C17 bond with elongation of its bond length (1.446 Å). The σ (O2–C19) is formed from sp^{1.68} hybrid on O2 (which is mixture of 37.32% s, 62.68% p atomic orbitals) and sp^{2.27} on C19 (30.61% s, 69.39% p). Furthermore, the increasing p characters on carbons C18 and C17 bond orbitals result in lengthening of the σ (C18–C17) bond than the other C–C bond lengths in the studied compound (Table 7). Decreased occupancy of the localized π (C18–C17) orbital in the Lewis structure, and increased occupancy of π^* (C18–C17) of the non-Lewis orbital and their subsequent impact on the molecular stability and geometry are also related with the pure p character of the two carbons C18 and C17 of the π (C18–C17) bond orbital as shown in Table 7. The intramolecular hyperconjugative interaction of the π electrons occurs from C7–C8 to π^* (C5–C6) (93.4 kJ/mol) leads to strong stabilization of the phthalonitrile moiety.

Finally, the NBO analysis clearly explains the evidence of the formation of weak H-bonded interaction between the LP(O) and σ^* (O–H) antibonding orbitals. The stabilization energies $E^{(2)}$ associated with hyperconjugative interaction LP1(O2) \rightarrow σ^* (C5–H3), is equal to 70.22 kJ/mol, which quantify the extend of intermolecular hydrogen bonding. Notwithstanding the energetic contribution for LP1(O2) \rightarrow σ^* (C16–H9) (6.93 kJ/mol) and LP1(O1) \rightarrow σ^* (C19–H10)

(2.17 kJ/mol) of hyperconjugative interaction is weak, these $E^{(2)}$ values are chemically significant and can be used as a measure of the intramolecular delocalization.

Conclusion

The 4-(1-formylnaphthalen-2-yloxy)phthalonitrile (1) was synthesized and characterized by IR, UV-vis, ^1H - ^{13}C NMR and X-ray single-crystal diffraction techniques. Crystal structure of title compound from the X-ray diffraction was found to be slightly different from its optimized counterparts. According to the computed results the phthalonitrile group is significantly twisted with respect to naphthalene group. The vibrational FT-IR spectra of compound were recorded and assigned with the aid of the experimental and computed vibrational wavenumbers and their PED. Potential energy distributions (PED) suggest that several normal modes are coupled in varying degrees. Therefore, the assignments made at higher level of theory with higher basis set with only reasonable deviations from the experimental values seem to be correct. The electronic absorption spectra calculations indicate that TD-HF method is not suitable to be used to study whereas TD-DFT method can predict the electronic spectra approximately. Molecular orbital coefficients analyses have shown that electronic spectra are assigned to $n \rightarrow \pi^*$ and $\pi \rightarrow \pi^*$. The magnetic properties of the title compound were observed and calculated. The chemical shifts were compared with experimental data, showing a very good agreement both for ^{13}C and ^1H . NBO results also suggest that there is a weak hydrogen bonding possibilities for title compound.

References

- [1] C.C. Leznoff, A.B.P. Lever, Phthalocyanines: Properties and Applications, VCH, New York, 1996. vols. 1–4.
- [2] N.B. McKeown, Phthalocyanine Materials: Synthesis, Structure and Function, Cambridge University Press, 1998.
- [3] D. Wöhrle, Macromol. Rapid Commun. 22 (2001) 68–97.
- [4] M.D. Halls, R. Aroca, D.S. Terekhov, A. D'Ascanio, C.C. Leznoff, Spectrochim. Acta Part A Mol. Biomol. Spectrosc. 54 (1998) 305–317.
- [5] A.C. Saladino, S.C. Larsen, Catal. Today 105 (2005) 122–133.
- [6] K.J. Almeida, Z. Rinkevicius, H.W. Hugosson, A.C. Ferreira, H. Agren, Chem. Phys. 332 (2007) 176–187.
- [7] J. Autschbach, T. Ziegler, Coord. Chem. Rev. 238–239 (2003) 83–126.
- [8] C.A. Venanzi, Reviews in Computational Chemistry, in: Kenny B. Lipkowitz, Donald B. Boyd (Eds.), vol. 8, VCH Publishers, 1996.
- [9] I. Ciofini, C.A. Daul, Coord. Chem. Rev. 238–239 (2003) 187–209.
- [10] C.A. Tsipis, Coord. Chem. Rev. 249 (2005) 2740–2762.
- [11] B.S. Jursic, J. Mol. Struct. Theochem. 417 (1997) 89–94.
- [12] M. Dinçer, N. Özdemir, N. Akdemir, M. Özdil, E. Açar, O. Büyükgüngör, Acta Crystallogr. E60 (2004) o896–o898.
- [13] J.G. Young, W. Onyebuagu, J. Org. Chem. 55 (1990) 2155–2159.
- [14] D.D. Perin, W.L.F. Armarego, Purification of Laboratory Chemicals, second ed., Pergamon, Oxford, 1980.
- [15] Stoe, Cie, X-AREA (Version 1.18) and X-RED (Version 1.04), Stoe & Cie, Darmstadt, Germany, 2002.
- [16] G.M. Sheldrick, SHELXS97 and SHELXL97, University of Gottingen, Germany, 1997.
- [17] K. Brandenburg, DIAMOND, Demonstrated Version, Crystal Impact GbR, Bonn, Germany, 2005.
- [18] M.J. Frisch, G.W. Trucks, H.B. Schlegel, G.E. Scuseria, M.A. Robb, J.R. Cheeseman, J.A. Montgomery Jr., T. Vreven, K.N. Kudin, J.C. Burant, J.M. Millam, S.S. Iyengar, J. Tomasi, V. Barone, B. Mennucci, M. Cossi, G. Scalmani, N. Rega, G.A. Petersson, H. Nakatsuji, M. Hada, M. Ehara, K. Toyota, R. Fukuda, J. Hasegawa, M. Ishida, T. Nakajima, Y. Honda, O. Kitao, H. Nakai, M. Klene, X. Li, J.E. Knox, H.P. Hratchian, J.B. Cross, C. Adamo, J. Jaramillo, R. Gomperts, R.E. Stratmann, O. Yazyev, A.J. Austin, R. Cammi, C. Pomelli, J.W. Ochterski, P.Y. Ayala, K. Morokuma, G.A. Voth, P. Salvador, J.J. Dannenberg, V.G. Zakrzewski, S. Dapprich, A.D. Daniels, M.C. Strain, O. Farkas, D.K. Malick, A.D. Rabuck, K. Raghavachari, J.B. Foresman, J.V. Ortiz, Q. Cui, A.G. Baboul, S. Clifford, J. Cioslowski, B.B. Stefanov, G. Liu, A. Liashenko, P. Piskorz, I. Komaromi, R.L. Martin, D.J. Fox, T. Keith, M.A. Al-Laham, C.Y. Peng, A. Nanayakkara, M. Challacombe, P.M.W. Gill, B. Johnson, W. Chen, M.W. Wong, C. Gonzalez, J.A. Pople, Gaussian 03, Revision B.05, Gaussian Inc., Pittsburgh, PA, 2003.
- [19] R. Dennington, I.I.T. Keith, J. Milliam, GaussView Version 4.1.2, Semichem Inc., Shawnee Mission, KS, 2007.
- [20] H.B. Schlegel, J. Comput. Chem. 3 (1982) 214–218.
- [21] R. Ditchfield, W.J. Hehre, J.A. Pople, J. Chem. Phys. 54 (1971) 724–728.
- [22] A.D. Becke, J. Chem. Phys. 98 (1993) 5648–5652.
- [23] C. Lee, W. Yang, R.G. Parr, Phys. Rev. B37 (1988) 785–789.
- [24] M. Dinçer, A. Agar, N. Akdemir, E. Agar, N. Özdemir, Acta Crystallogr. E60 (2004) o79–o80.
- [25] T. Akbal, N. Akdemir, M. Özil, E. Agar, A. Erdönmez, Acta Crystallogr. E61 (2005) o1121–o1122.
- [26] S.Y. Lee, Bull. Korean Chem. Soc. 19 (1998) 93–116.
- [27] S.Y. Lee, B.H. Boo, J. Phys. Chem. 100 (1996) 15073–15078.
- [28] S.Y. Lee, B.H. Boo, J. Phys. Chem. 100 (1996) 8782–8785.
- [29] M. Kurt, S. Yurdakul, J. Mol. Struct. 654 (2003) 1–9.
- [30] F.F. Jian, P.S. Zhaou, Q. Yu, Q.X. Wang, K. Jiao, J. Phys. Chem. A108 (2004) 5258–5267.
- [31] J.A. Pople, H.B. Schlegel, R. Krishnan, D.J. Defrees, J.S. Binkley, M.J. Frisch, R.A. Whiteside, R.F. Hout, W.J. Hehre Int. J. Quantum Chem. Quantum Chem. Symp. 15 (1981) 269–278.
- [32] G. Varsanyi, Assignments for vibrational spectra of seven hundred benzene derivatives, vol. 1/2, Academic Kiado, Budapest, 1973.
- [33] S. Mohan, R. Murugan, Indian J. Pure Appl. Phys. 31 (1993) 496–499.
- [34] R.M. Silverstein, G.C. Bassler, T.C. Morrill, Spectroscopic Identification of Organic Compounds, 4th ed., JohnWiley and sons, New York, 1981.
- [35] D. Lin-Vien, N.B. Colthup, W.G. Fateley, J.G. Grasselli, The Handbook of Infrared and Raman Characteristic Frequencies of Organic Molecules, Academic Press, Boston, MA, 1991.
- [36] A. Coruh, F. Yilmaz, B. Sengez, M. Kurt, M. Cinar, M. Karabacak, Struct. Chem. 22 (2011) 45–56.
- [37] K. Zeng, K. Zhou, W.R. Tang, Y. Tang, H.F. Zhou, T. Liu, Y.P. Wang, H.B. Zhou, G. Yang, Chin. Chem. Lett. 18 (2007) 523–526.
- [38] K. Zeng, K. Zhou, S. Zhou, H. Hong, H. Zhou, Y.W.P. Miao, G. Yang, Eur. Polym. J. 45 (2009) 1328–1335.
- [39] R. Meenakshi, J. Lakshmi, S. Gunasekaran, S. Srinivasan, J. Mol. Simul. 36 (2010) 425–433.
- [40] S.I. Gorelsky, SWizard Program Revision 4.5, <<http://www.sg.chem.net/>>, University of Ottawa, Ottawa, Canada, 2010.
- [41] K. Fukui, Science 218 (1982) 747–754.
- [42] A.E. Reed, L.A. Curtiss, F. Weinhold, Chem. Rev. 88 (1988) 899–926.